Characterization of a Fluoropolymer Thin Film Synthesized in a Photoexcited Radio-Frequency Plasma

Iwao Sugimoto

NTT Applied Electronics Laboratories, Midori-cho, Musashino-shi, Tokyo 180, Japan

Received June 11, 1990; Revised Manuscript Received September 13, 1990

ABSTRACT: The effects of ultraviolet light irradiation during radio-frequency plasma fluoropolymer sputtering on the structure of a deposited polymer film was investigated by well-established chemical analytical techniques. Thermal analyses reveal that thermal stability is enhanced by photoassisted effects. Elemental and spectroscopic analyses, such as magnetic resonance and X-ray photoelectron spectroscopies, clarified that the photoassisted effect on the molecular structure is an enhancement of unsaturated carbons through C–F bond cleavage by electronic excitation. These unsaturated bonds result in radical spins and induce a conjugated structure. This effect is also supported by the results of ultraviolet–visible and infrared spectroscopies.

Introduction

Plasma processing has enormous potential for producing useful organic materials that cannot be prepared by the usual chemical reactions. However, it has not been given much attention in synthetic chemistry, because of the difficulty in characterizing plasma products by well-established chemical analyses. This problem is primarily due to the complete insolubility of these products. Structural characterization of polymer films produced in plasma (plasma polymer films) has been mainly performed by infrared (IR) or X-ray photoelectron spectroscopies (XPS). These methods are not powerful enough to reveal molecular structure in detail. Generally, beam analytical methods, such as Auger electron spectroscopy (AES) and secondary ion mass spectroscopy (SIMS), are available for the analysis of such insoluble high molecular weight polymer films. However, these analytical methods provide only information about the near surface. Moreover, their analytical probes are destructive to plasma polymer films, which include unstable moieties such as radical sites and hindered and weak bonds. There is also the possibility of undesirable structural change in the films through bond cleavage by the beam probes (energetic ion,[1] electron,[2] and X-ray[3,4] beams).

Spectroscopic analyses, such as IR, ultraviolet–visible (UV–vis), nuclear magnetic resonance (NMR), and electron spin resonance (ESR) spectroscopies, are methodologically and logically well-established as chemical analytical techniques. Generally, these spectroscopic analyses are slightly destructive, due to relatively low energy excitation sources. Chromatography, used in combinations with elemental analysis, is useful in elucidating the components of the bulk film materials. However, it is hard to obtain plasma polymer of sufficient quantity to be chemically analyzed, due to the low production rate of plasma processing. Moreover, their insolubility, due to high molecular weight and cross-linked structure, enormously increases the difficulty of the chemical analysis. These difficulties prevent persuasive chemical analyses for the bulk of plasma polymer films, especially fluoropolymer films. However, there are some reports on characterizations of plasma polymers from the chemical aspects.[5–10]

We studied plasma polymer film synthesis by fluoropolymer sputtering in radio-frequency (rf) plasma excited by ultraviolet (UV) light[11] and a magnetic field.[12] Electronic transition of the C_xF_y species, which are generated in plasma by energetic electron and ion bombardments to fluoropolymers as a result of UV light absorption, should affect the molecular structure of plasma products. The effects of photoexcitation on the molecular structure of plasma polymer film are carefully examined by chemical and beam analyses in this study. In general, the molecular structure of polymer-sputtered film involves radical sites as bond defects that are unlikely to be quenched under the vacuum conditions of plasma processing. Bond formation between reactive radical sites can result in multiple carbon bonds and a cross-linking structure. When plasma products are exposed to air, these active radical sites may interact with radically reactive species, such as oxygen and hydrocarbons. In the characterization of the structure of plasma polymer film, one of the essential problems is to elucidate the behavior of these radical sites in air. The solution of these characterization problems should lead to modifications of plasma processing that produce excellent functional materials and reduce the disadvantages of plasma product, such as aging.[13–16]

Experimental Section

Plasma polymer films were produced by 13.5-MHz rf sputtering of poly(chlorotrifluoroethylene) (PCTFE) under low-pressure 300-W mercury lamp irradiation (185 and 254 nm). The plasma reactor (photoassisted sputtering equipment) configuration and film preparation procedure have been previously described.[11] Fluoropolymer films were deposited on silicon wafers and quartz substrates. It is conceivable that halocarbons, which arise from decomposition of PCTFE, constitute a large proportion of the plasma species. To prevent surface contamination and reaction with reactive species in air, all deposited films were stored in a vacuum drying box under a pressure of 40 mmHg after completion of plasma processing.

Elemental analysis was carried out with a Yanagimoto CHN corder MT-3 and Heraeus CHN-O Rapid autoanalyzer to determine the C, H, N, and O concentrations. The sample furnace was kept above 930 °C during operation, and no ash was detectable after the measurement in either piece of equipment. F and Cl concentrations were determined by flask combustion in oxygen followed by potentiometric titration by $AgNO_3$ for F^- and ion-exchange chromatography (Yokogawa Model-IC200) for Cl^-.

IR and UV–vis spectra were measured with a Digilab FTS-60 and a Hitachi U-3400 spectrophotometer. IR spectra were obtained by a microtransmission method in which the film materials were scraped down from silicon wafer onto a KRS-5 disk. UV–vis measurements were also carried out by the transmission method, using as-deposited films on quartz substrates.

0024-9297/91/2224-1480$02.50/0 © 1991 American Chemical Society

The ^{19}F-NMR spectra were recorded on a JNM-GX400, and chemical shift values are given in parts per million (ppm) relative to internal $CFCl_3$ in acetone-d_6 solvent. The measured frequency was 376.2 MHz, the flip angle was 30°, and the pulse delay time was 5 s. The plasma polymer films deposited on silicon wafers became soluble if they were submerged for 4 h and ultrasonics were used. All of these measurements were performed after the subsequent solvent exchange of the deuteriated solvent.

XPS measurements were performed with a VG Microlab MK2 using Mg Kα radiation as the excitation source. The chamber pressure during operation was 6×10^{-10} Torr, and the incident angle between the liberated photoelectron and film surface was 90°. All binding energies were calibrated to compensate for charging, on the basis that a simple Gaussian F_{1s} peak was set to 689 eV, which is representative of C–F systems. With use of this value, the binding energy of the CF_3 carbon, which was hardly affected by neighboring groups, was calibrated to the reasonable value of nearly 293.8 eV in all cases. The sensitivity factors used for elemental ratio calculation were based on the Perkin-Elmer Corp. data book value; C_{1s}, 0.205; F_{1s}, 1.00; Cl_{2p}, 0.48.[17]

ESR spectra were recorded on a JES-FE3XG using the films deposited on quartz substrates. The G values and spin densities were determined by comparison with Mn^{2+}/MgO used as an external reference. The measurements were made in an argon atmosphere at 25, 150, 280, and 350 °C.

Differential scanning calorimetry (DSC) and thermogravimetry (TG) analyses were carried out using Shimadzu DSC-50 and TGA-50 coupled with a TA-50 thermal analysis data station. The heating rate was 10 °C/min in both cases. Al_2O_3 was used as an external reference for the DSC measurement. Inert gas exchange in the aluminum pan was not carried out. TG measurements were performed under nitrogen gas flow.

Solid-state ^{13}C NMR spectroscopy was performed with a JNM-GSX270. The resonance frequency was 67.94 MHz, and the pulse width was 4.0 μs. Chemical shift values are given in parts per million (ppm) relative to the internal reference of silicon rubber [$(-Si(CH_3)_2-)_n$]. The measurements were performed by pulse saturation/magic angle spinning (PS/MAS) and cross polarization/magic angle spinning (CP/MAS) methods. A measurement sample of approximately 170 mg scraped from the silicone wafer substrate was used.

Results and Discussion

The thermal analyses should precede the temperature-dependent analysis. TG and DSC curves of fluoropolymer films, which are produced by photoassisted sputtering (photoassisted film) and by conventional sputtering (conventional film), are depicted in Figure 1. The TG curves suggest that both films begin to lose weight by release of degradation products at around 180 °C. Thermal weight loss of conventional film begins at a lower temperature with a high rate compared to the photoassisted film. Extremely weak exothermal peaks on DSC curves in both films can be also detected around 180 °C. They are probably due to the thermal decomposition. Corresponding to the results of TG analysis, this thermal decomposition peak of conventional film appears at a lower temperature than for the photoassisted film. Neither DSC curve indicates the melting points, which should be suggested by endothermal peaks.

In general, plasma-produced fluoropolymers contain large numbers of radical sites[9,18,19] that are stable in air because of the complicated structure shields against reactive species and the hyperconjugation of unsaturated fluorocarbon systems. The ESR spectra at 25 °C of both films are shown in Figure 2. Broad resonance curves without fine structure, which are typical ESR signals of plasma-produced polymers, are observable in both spectra. These broad curves are caused by the complicated carbon frameworks including the cross-linking and branched-chain structures considerably. The G value is 2.0038 for the photoassisted film and 2.0022 for the conventional

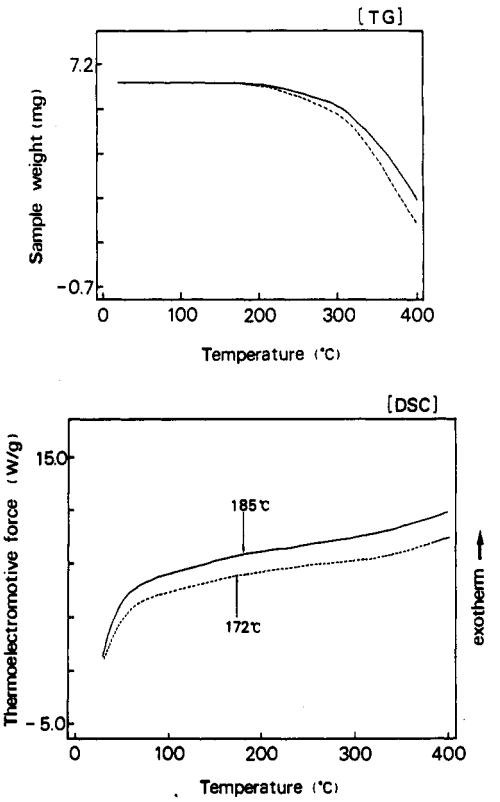

Figure 1. Thermal analyses of TG and DSC curves from 25 to 400 °C: (—) photoassisted film; (- - -) conventional film.

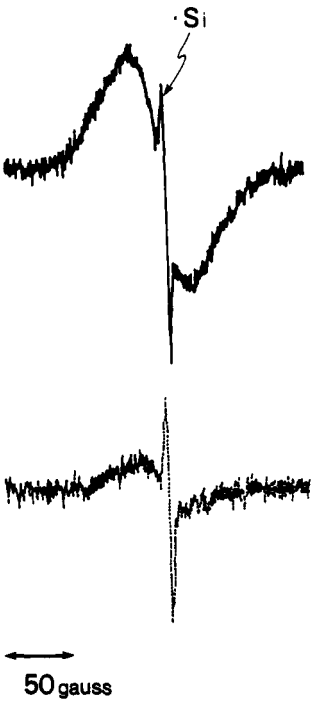

Figure 2. ESR spectra measured for the films deposited on quartz substrate in argon at 25 °C; (—) photoassisted film; (- - -) conventional film.

film. The temperature-dependent spin density and line width are shown in Figure 3. For photoassisted film, both spin density and line width decrease as temperature increases up to 280 °C. Considering the results of thermal analyses, these decreases are attributed to active motion of radical sites due to thermal effects. On the contrary, the spin density of conventional film increases, especially at 280 °C. However, the line width decreases as for the photoassisted film. This is probably caused from bond

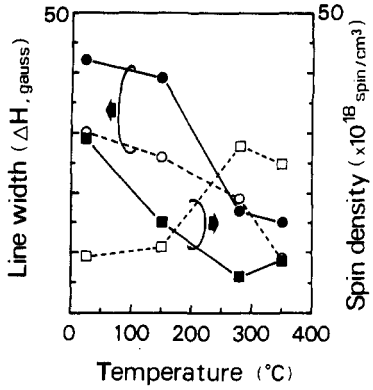

Figure 3. Temperature-dependent spin density and line width estimated from ESR analysis: (—) photoassisted film; (- - -) conventional film.

Table I
Chemical Elemental Analysis (percent) for C, F, Cl, and O

	C	F	Cl	O
photoassisted	32.0	35.6	14.1	18.2
conventional	30.9	38.1	13.8	17.3

cleavage by thermal degradation resulting in a large number of mobile radical species of lower molecular weight. Both films turn from dark yellow to dark brown after the 350 °C measurement. This color change suggests carbonization by vigorous thermal decomposition. Sharp signals appearing in these broad curves can be assigned to the E′ center of silicon radicals on the basis of their G values, which are likely to originate at the surface of quartz substrate. The signal intensity diminished as temperature increased, becoming almost invisible at 280 °C. This may be due to radical coupling with the reactive and mobile radical sites produced by thermal decomposition of film molecules at the film/substrate interface.

As described above, these fluoropolymers contain stable radical sites with a high density in the solid state. These radical sites, however, may become reactive in solution, owing to reduction of the shielding effect that is effective in solid state. Therefore, there is a possibility of structural change of film molecules by radical reaction in solution. Thus, it is desirable that structural analyses be carried out in the solid state, because the film structure as deposited is preserved.

Elemental analysis was a fundamental of characterization of molecular structure. The values of atomic concentrations, which are mean values of four measurements, are summarized in Table I. These results are particularly surprising in view of the fact that both films contain oxygen at the concentration of about 18%. This oxygen incorporation is probably from oxygen in the air, because there is no oxygen source in the reaction chamber. Spin–spin interaction between radical sites in film molecules and oxygen probably plays an important role in air after the film deposition process. No significant difference between the two films is observable in these results of elemental analyses.

XPS analysis is not sufficiently effective to determine detailed structure, such as clarification of the immediate CF_x environments, in fluoropolymer characterization. Especially, information from only the near surface, which is likely to be disturbed by surface contamination, is an essential problem in characterization of "bulk" structure. However, XPS analysis is certainly one of the most effective methods of characterizing plasma polymers, because operation does not require further treatment of as-deposited films. Inert gas ion sputtering is generally

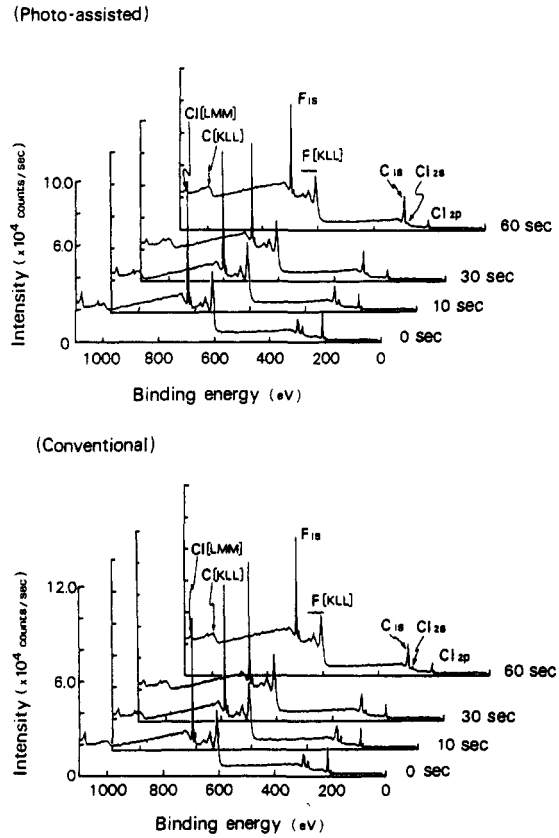

Figure 4. Full-region XPS spectra depended on Ar^+ ion sputtering time.

used to remove surface contamination. Structural change by ion bombardment should be given special attention in organic material analysis. Structural change by low-energy (1 keV) Ar^+ ion bombardment was investigated.[1] XPS spectral dependence on Ar^+ ion sputtering time is shown in Figure 4. Even at the film surface, oxygen is almost undetectable at concentrations of less than 1% in both films. The time the films are exposed to air after completion of deposition process is minimized. This apparent oxygen nonincorporation conflicts with the results of the elemental analysis shown in Table I. A plausible explanation for this is that the ultrahigh vacuum and X-ray irradiation during XPS measurement release oxygen from the film surface. Oxygen ions (m/e = 16) are also not detectable in secondary ion mass spectroscopy (SIMS) measurements. Therefore, it is probable that the films incorporate oxygen, which is detectable in elemental analysis, so weakly that oxygen is evacuated under an ultrahigh vacuum of less than 10^{-9} Torr. This explanation is supported by the undetectable ESR signals of peroxy radicals (ROO•), which should be formed by the bond formation between radical sites and adsorbed oxygen. These radical sites trapped near the top surface are stable in air because they are protected from oxygen by shielding effect of the closely cross-linked polymer networks at the top surface. Oxygen incorporation may be attributed to the weak spin–spin interaction between radical sites and triplet oxygen molecules.

Elemental ratios (X/C, X = F, Cl) and C_{1s} XPS spectral dependence on Ar^+ sputtering time are summarized in Figures 5 and 6. The F/C ratios of conventional and photoassisted films at the surface are 0.90 and 0.84. The slightly lower value of photoassisted film may be attributed to a C–F bond cleavage induced by UV irradiation, corresponding to higher radical concentration (Figure 3). Low halogenation (F + Cl/C ratio under 2.0) of film molecules

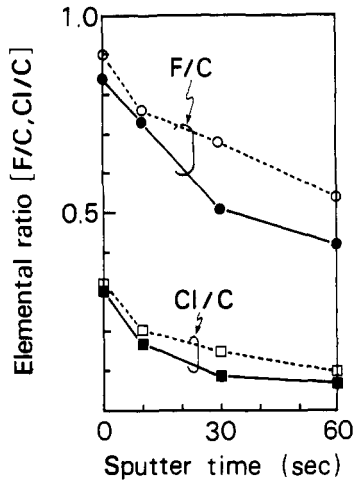

Figure 5. Elemental ratios (F/C, Cl/C) vs Ar^+ ion sputtering time in XPS spectra: (—) photoassisted film; (- - -) conventional film.

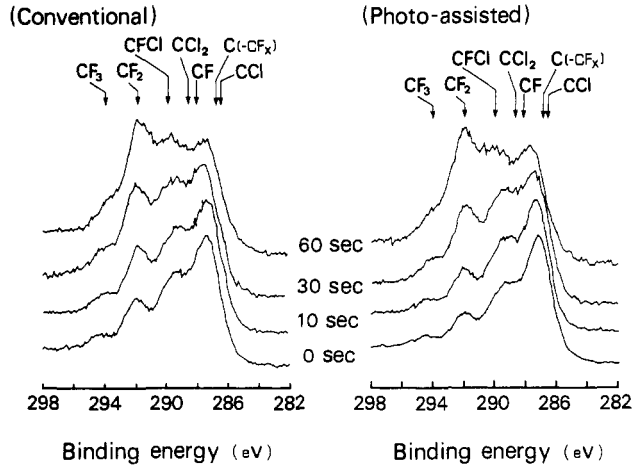

Figure 6. C_{1s} XPS spectra vs Ar^+ ion binding energy.

is confirmed even at the surface, where halogen concentration is likely to be maximum without further defluorination by an exposure in plasma. This result suggests that the carbon framework involves considerable crosslinking and unsaturated bonds together with dangling bonds (radical sites). Comparing photoassisted film with conventional film, halogen atoms are more preferentially sputtered out in photoassisted film, suggested by the steeper decrease of the X/C ratio curve with sputtering time. Signal intensities of highly halogenated moieties (CF_3, CF_2, and CFCl), which are likely to be near the surface, decrease steeply with sputtering time (Figure 6). On the contrary, the signal intensities of the lowly halogenated moieties (CF, CCl, and $C(CF_x)$) are relatively enhanced. This reduction in intensity of highly fluorinated moieties induces the decrease in the X/C ratio with sputtering time. The steep decrease in the CF_3 and CF_2 signals suggests that fluorine atoms are preferentially sputtered out. This may be caused by the outer configuration of fluorines wrapping the inner carbon chain, which are likely to be exposed to the Ar^+ beam.[1]

To reveal the photoassisted effects on C–F bond strength, IR spectra with absorbance scales are shown in Figure 7. Fluorinated C=C stretching bands are weakly observed around 1680 cm^{-1}, and this band intensity is slightly increased by the photoassisted effect, as shown previously.[11] The peak of the C–F stretching band around 1200 cm^{-1} shifts somewhat to lower wavenumbers for the photoassisted film than for the conventional film. This C–F stretching band shift suggests lower fluorination and

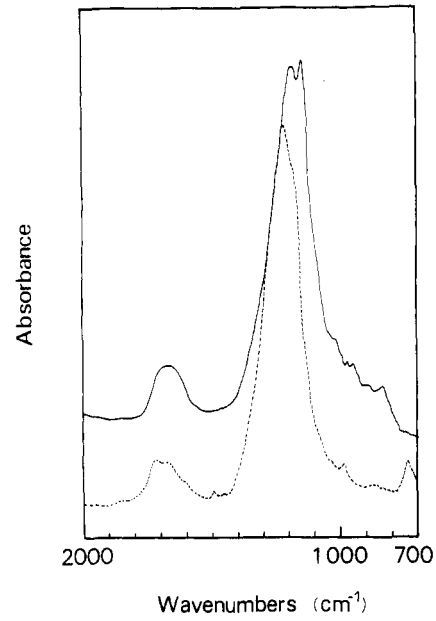

Figure 7. IR spectra measured for the film materials scraped on a KRS-5 disk: (—) photoassisted film; (- - -) conventional film.

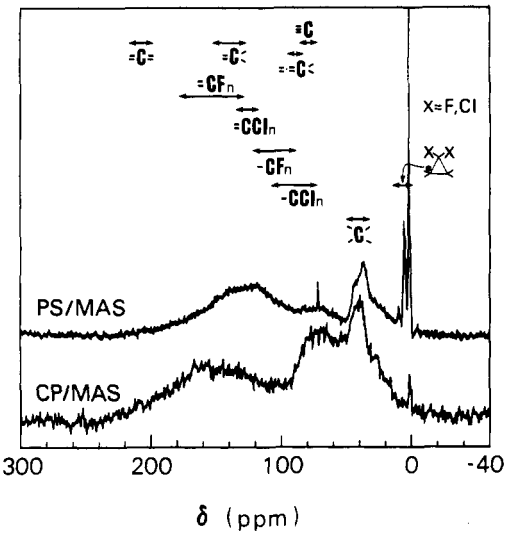

Figure 8. Solid-state ^{13}C NMR spectra by pulse saturation/magic angle spinning (PS/MAS) and cross polarization/magic angle spinning (CP/MAS) methods.

a reduction of the C–F bond strength of CF_x moieties in the photoassisted film. These suggestions correspond to the lower F/C ratio and its steeper decrease by Ar^+ sputtering in photoassisted film (Figure 5).

Nuclear magnetic resonance spectroscopy is a powerful method for structural analysis. High-resolution solid-state NMR spectroscopy has developed greatly in the past decade.[10,20,21] Solid-state ^{13}C NMR spectra of the conventional film are shown in Figure 8. Complicated spin coupling, reduction of relaxation time by unpaired electrons (radicals), and interlocking polymer structures induce the signal broadening shown in these spectra. The PS/MAS spectrum mainly reflects mobile structures, and the CP/MAS spectrum mainly reflects rigid structures. The PS/MAS spectrum can be roughly divided into four regions. Relatively sharp signals appear from 0 to 10 ppm. They are assigned to bridgehead sp_3 carbons of cyclopropane rings, which should be produced by addition of CF_2 carbene to C=C.[22-24] The existence of CF_2 carbene in the reaction chamber and of C=C in film molecules is confirmed by plasma emission spectroscopy[25] and IR

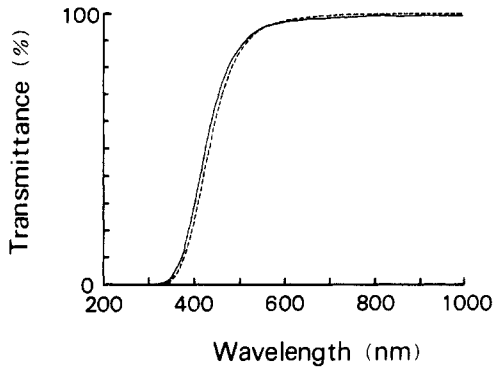

Figure 9. UV-vis spectra measured for the films deposited on quartz substrate: (—) photoassisted film; (- - -) conventional film.

spectroscopy (Figure 7). The complicated band from 10 to 50 ppm is assigned to unfluorinated sp_3 carbons constituting the carbon framework. The weak band from 50 to 90 ppm involves many candidates, such as sp carbon, allene, *C*F, and *C*Cl_x. The widely broad band from 90 to 200 ppm can be assigned to sp_2 carbons, *C*F_3, and *C*F_2. Unfortunately, signals arise from the highly fluorinated moieties (CF_3, CF_2), and sp_2 carbons are indistinguishable, owing to their similar chemical shift values. Besides these broad bands, this PS/MAS spectrum includes some sharp lines, which originate in extremely motive moieties species, such as the molecules with low molecular weight. The relatively sharp band, originating in the bridgehead carbon of cyclopropane rings, is lower in the CP/MAS spectrum than in the PS/MAS spectrum. In contrast, the complicated band from 50 to 90 ppm is enhanced. Therefore, this band may mainly originate in unsaturated carbons composing the rigid framework. In addition, the band intensity around 120 ppm is reduced. This band is considered to arise from the mobile $CF_{2,3}$ moieties.

UV-vis spectra of the films deposited on quartz substrates are shown in Figure 9. They do not exhibit the characteristic band structure. The edge of the absorption curve extends to about 550 nm in both spectra. This extension of the absorption region suggests that these films are constructed from a carbon framework involving considerably conjugated systems. We evaluate the extent of conjugation in comparison with the simple conjugated systems, such as linear polyenes [R(CH=CH)$_n$R] and polyacenes:

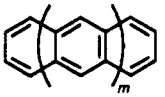

The absorption edge of 550 nm corresponds to the π-π^* transition energy of dodecahexene (n = 6) and is directly between the lowest transition energy of naphthalene (m = 1) and that of naphthacene (m = 2). The absorption curve of the conventional film shifts slightly toward longer wavelengths than does that of the photoassisted film. Lone pairs on halogen atoms conjugating with unsaturated carbon systems may play an important role in the bathochromic effect, which results from the slightly higher concentration of halogen atoms in conventional film.

A homogeneous solution is one of the most important factors in obtaining a high-resolution NMR spectrum, especially in NMR analysis of polymers. In solutions where radical sites of the films can react with solvent molecules, structural changes may result from radical reactions. Especially in halogenated solvents, significant alternation of film molecular structure by halogen extraction from the solvent molecules is possible. However, it is unlikely

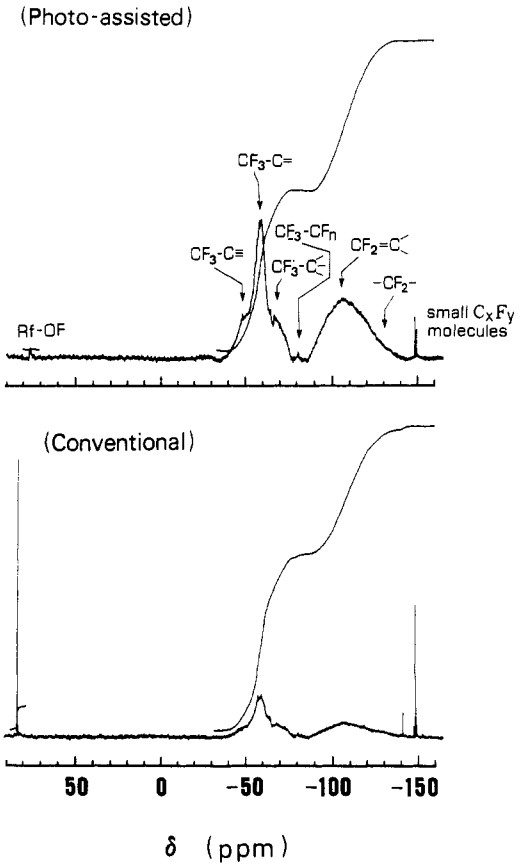

Figure 10. ^{19}F NMR spectra measured in acetone-d_6 with $CFCl_3$ as an internal reference.

Table II
Area Ratios (percent) of Each Component Constituting the CF_3 Band in ^{19}F NMR Spectra

	$CF_3C\equiv$	$CF_3C=$	CF_3C-	CF_3CF_n
photoassisted	19.1	62.3	17.0	1.6
conventional	14.0	60.4	19.0	6.6

that hydrogenation of these radical sites will affect the structure of the halocarbon framework. Thus, a hydrogen-donating solvent is desirable for structural analyses in solution. Acetone is the most effective solvent, because of its high solubility and the low reactivity of the acetyl radical produced by hydrogen extraction.

^{19}F NMR spectra of the films in acetone-d_6 are shown in Figure 10. They roughly consist of two broad bands and some lines. Broad bands originate in polymeric molecules constituting the films. A complicated band from −35 to −85 ppm arises from *C*F_3, and a simple band from −85 to −145 ppm arises from *C*F_2. The CF band, which should appear in the lower ppm region, is not detectable in either spectra. This may be caused by the extreme broadening of this band due to complicated spin coupling and the extremely low concentration of the CF moiety among the film components. The CF_3 band can be divided into four components, assigned to *C*F_3C≡, *C*F_3C=, *C*F_3C–, and *C*$F_3CF_{1,2}$ in order from low to high magnetic field. The area ratios of these CF_3 peaks are summarized in Table II. Note that CF_3 is mainly attached to unsaturated carbons. These results suggest that the photoassisted film contains unsaturated carbons in higher concentration and fluorinated sp_3 carbon in lower concentration than the conventional film. The CF_2 band mainly consists of the sp_2 CF_2 (*C*F_2=C) in both films. The sp_2 C/sp_3 C ratio is larger in the photoassisted film. This component division of CF_3 and CF_2 bands revealed the existence of an

unsaturated carbon with a high concentration in both films. This concentration is higher in the photoassisted film than in the conventional film. It is conceivable that this high concentration of unsaturated carbons induces the extension of the absorption edge to a higher wavelength at 550 nm, even in the halocarbon systems.

A sharp line appearing around 80 ppm probably arises from fluorine atoms bonded with heteroatoms. They should be included in the sample solvent and are probably oxygen. However, this type of oxygen is indistinguishable from either fluorinated acetone solvent or oxygenated film molecules. Some of the sharp lines appearing between −140 and −150 ppm probably originate in mobile molecules with low molecular weight. The intensities of these sharp lines are higher for the conventional film than for the photoassisted film. This suggests that polymerization is enhanced by the photoassisted effect, producing a film that involves few reactive sites with oxygen and low molecular weight species (Figure 10). The area ratio of the CF_2 band is larger in photoassisted film than in conventional film. In contrast, the area ratio of low molecular weight species is the opposite for both films. Therefore, these results suggest that the concentration increase of sp_2 CF_2 moieties in the films correlates with the propagation of polymerization, even involving radical sites. This may originate from the stabilization of film molecular structure by conjugated structures.

If the oxygenated fluorine (Rf-OF) line appearing around 80 ppm arises from film molecules, radical sites of the films should play an important role in oxygenation. It seems strange that radical spin density is higher in photoassisted film than in conventional film (Figure 3). A plausible explanation is that in photoassisted film, the concentration of stable and unreactive radicals that conjugate with π systems is higher than in conventional film, as shown in ^{19}F NMR and IR analyses. The shielding effect of the complicated structure of film molecules enhances this stabilization of radicals in the solid state. Radical spin density is reduced by radical coupling through activation of chain motion as the temperature increases in the temperature-dependent ESR measurements (Figure 3). On the contrary, the lower concentration of conjugated systems, which contributes to stabilization of the radicals, cannot reduce their reactivity in the conventional film. Therefore, these reactive radicals should interact hardly with oxygen, leading to the oxygen incorporation. This is suggested by elemental analysis and the ^{19}F NMR spectrum and by the enhancement of spin density by increasing temperature (Figure 3) through reaction with absorbed oxygen and thermal decomposition of the polymeric chain.

Conclusion

The structures of polymers produced by fluoropolymer (PCTFE) sputtering in rf plasma were analyzed by well-established chemical analytical methods, revealing the effects of UV irradiation of the rf plasma on the structure of plasma products in detail. Thermal analyses (TG and DSC) demonstrated that photoassisted film is more stable against thermal decomposition than conventional film. ESR analysis clarified the high-spin density in both films and showed that spin density is increased by the photoassisted effect. Temperature-dependent ESR spectra suggested that these radicals and film molecules are more stable in photoassisted film than in conventional film. Elemental analysis indicated oxygen icnorporation in both films at a concentration of about 18%. The source of the oxygen is probably air, because other spectroscopic anal-

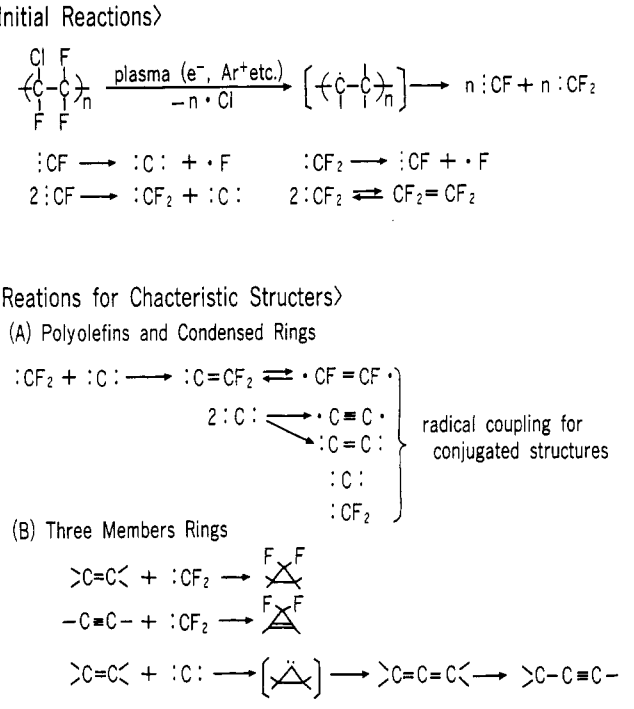

Figure 11. Plausible reaction mechanism into the characteristic film structures.

yses (XPS and SIMS) in ultrahigh vacuum could not detect the incorporation of oxygen. XPS analysis showed that the F/C ratio is slightly higher in photoassisted film than in conventional film. These results are derived from C–F bond cleavage by UV light absorption, leading to reduction of fluorine concentration and enhancement of spin density in photoassisted film.

Solid-state ^{13}C NMR spectroscopy for conventional film revealed the existence of cyclopropane rings and unfluorinated sp_3 carbons making up the carbon framework. In addition, unsaturated carbons are directly observable in PS/MAS and CP/MAS spectra. Unexpected prolongment of the UV–vis absorption curve edge to 550 nm suggests considerable amounts of unsaturated carbons (sp_2 C and sp C) constituting the film molecules. ^{19}F NMR spectroscopy was performed in acetone-d_6 solvent, which should hardly affect the halocarbon framework, even though the hydrogenation reaction would take place in solution. Signals arise from CF_3 and CF_2 moieties, which bond with unsaturated carbons, are detectable as a broadening band. The area ratios of both CF_2/CF_3 and unsaturated carbon/saturated carbon are higher in photoassisted film than in conventional film. Some sharp lines, which originate in oxygen-bonded fluorines and fluorocarbons with lower molecular weight, were observed among these broad bands. The intensity of these lines may indicate incomplete polymerization and the radical reactivity in films. This indication is weaker in the photoassisted film than in the conventional film. On the whole, it is clarified that film stability is enhanced by photoassisted effects on availability in the construction of conjugated structures.

Plausible mechanism of constructing characteristic film structures is summarized in Figure 11, based on the spectroscopic informations. PCTFE molecules in a rf discharge should be fully decomposed into the halocarbon radicals and carbenes. Among these reactive species, atomic carbon (:C:) and difluoromethylene ($:CF_2$) are dominant products, expected from their relatively high stability and behaviors of fluorocarbon radicals.[5,26] The adducts of atomic carbon and difluoromethylene are

probably in an equilibrium between difluorocarbene and difluorobiradical, whereas acetyl biradical and ethylbicarbene are likely to be produced by a disproportionation reaction of atomic carbons. These alkenyl and alkynyl radical species should greatly contribute to the construction of the conjugated frameworks, such as the polyolefinic and condensed aromatic ring structures that were suggested by NMR, IR, and UV–vis analyses. In addition, fluorocyclopropanes are postulated to arise by addition of CF_2 carbene and CF triradical to the unsaturated bonds.[24,27,28] It is probable that allenic and propynic structures are produced by the collapse of unstable cyclopropylidene as an adduct of atomic carbon and olefins.[29-31] UV light irradiation in plasma should induce photochemical reaction such as bond fission and cycloaddition, which induce the branched chain and cross-linking structures.[32,33]

Acknowledgment. This work greatly depended on the instructive suggestions of Hon. Prof. Teruo Matsuura of Kyoto University and Assoc. Prof. Shojiro Miyake of the Nippon Institute of Technology. I express my grateful acknowledgment to them for their helpful discussions.

References and Notes

(1) Takahagi, T.; Ishitani, A. *Macromolecules* **1987**, *20*, 404.
(2) Pepper, S. V. *J. Appl. Phys.* **1974**, *45*, 2947.
(3) Wheeler, D. R.; Pepper, S. V. *J. Vac. Sci. Technol.* **1982**, *20*, 226.
(4) Rye, R. R.; Martinez, R. J. *J. Appl. Polym. Sci.* **1989**, *37*, 2529.
(5) Mathias, E.; Miller, G. H. *J. Phys. Chem.* **1967**, *71*, 2671.
(6) Lo, E. S.; Osborn, S. W. *J. Org. Chem.* **1970**, *35*, 935.
(7) Kobayashi, H.; Bell, A. T.; Shen, M. *Macromolecules* **1974**, *7*, 277.
(8) Tibbitt, J. M.; Shen, M.; Bell, A. T. *J. Macromol. Sci., Chem.* **1976**, *A10*, 1623.
(9) Hozumi, K.; Kitamura, K.; Kitade, T. *Bull. Chem. Soc. Jpn.* **1981**, *54*, 1392.
(10) Kaplan, S.; Dilks, A. *J. Appl. Polym. Sci., Appl. Polym. Symp.* **1984**, *38*, 105.
(11) Sugimoto, I.; Miyake, S. *J. Appl. Phys.* **1988**, *64*, 2700.
(12) Sugimoto, I.; Miyake, S. *J. Appl. Phys.* **1990**, *67*, 2093.
(13) Yasuda, H.; Bumgarner, M. O.; Marsh, H. C.; Morosoff, N. *J. Polym. Sci., Polym. Chem. Ed.* **1976**, *14*, 195.
(14) Wrobel, A. M. *J. Macromol. Sci., Chem.* **1985**, *A22*, 1089.
(15) Biederman, H.; Martinu, L.; Nespurek, S. Proc. 8th Int. Symp. Plasma Chem. (ISPC-8/Tokyo); IUPAC: Tokyo, 1987; Vol. 3, pp 1364–1367.
(16) Morra, M.; Occhiello, E.; Marola, R.; Garbassi, F.; Humphrey, P.; Johnson, D. *J. Colloid Interface Sci.* **1990**, *137*, 11.
(17) Warner, C. D.; Rigg, W. M.; Davis, L. E.; Moulder, J. E.; Muilenberg, G. E. *Handbook of X-ray Photoelectron Spectroscopy*; Perkin-Elmer Corp.: Eden Prairie, MN, 1979.
(18) Morita, S.; Mizutani, T.; Ieda, M. *Jpn. J. Appl. Phys.* **1971**, *10*, 1275.
(19) Millard, M. M.; Windle, J. J.; Pavlath, A. E. *J. Appl. Polym. Sci.* **1973**, *17*, 2501.
(20) Fleming, W. W.; Fyfe, C. A.; Lyerla, J. R.; Vanni, H.; Yannoni, C. S. *Macromolecules* **1980**, *13*, 460.
(21) Dec, S. F.; Wind, R. A.; Maciel, G. E. *Macromolecules* **1987**, *20*, 2754.
(22) Rahman, M.; Mckee, M. L.; Shevlin, P. B. *J. Am. Chem. Soc.* **1986**, *108*, 6296.
(23) Siddiqui, S.; Cais, R. E. *Macromolecules* **1986**, *19*, 595.
(24) Thomsen, M. W.; Katz, S. A.; Horenkamp, E. C.; Heidig, K. S. *Macromolecules* **1989**, *22*, 481.
(25) Sugimoto, I.; Miyake, S. *J. Appl. Phys.* **1989**, *65*, 4639.
(26) Mastrangelo, S. V. R. *J. Am. Chem. Soc.* **1962**, *84*, 1122.
(27) Siddiqui, S.; Cais, R. E. *Macromolecules* **1986**, *19*, 595.
(28) Rahman, M.; Mckee, M. L.; Shevlin, P. B. *J. Am. Chem. Soc.* **1986**, *108*, 6296.
(29) Blaxell, D.; Mackay, C.; Wolfgang, R. *J. Am. Chem. Soc.* **1970**, *92*, 50.
(30) Skell, P. S.; Villaume, J. E.; Plonka, J. H.; Fagone, F. A. *J. Am. Chem. Soc.* **1971**, *93*, 2699.
(31) Dilks, A.; Kay, E. *Macromolecules* **1981**, *14*, 855.
(32) Corbin, G. A.; Cohen, R. E.; Baddour, R. F. *Macromolecules* **1985**, *18*, 98.
(33) Munro, H. S.; Till, C. *J. Polym. Sci., Polym. Chem. Ed.* **1988**, *26*, 2873.

Registry No. PCTFE, 9002-83-9.